RhoA as a Signaling Hub Controlling Glucagon Secretion From Pancreatic α-Cells

Xue Wen Ng, Yong Hee Chung, Farzad Asadi, Chen Kong, Alessandro Ustione, and David W. Piston

Diabetes 2022;71:2384–2394 | https://doi.org/10.2337/db21-1010

Glucagon hypersecretion from pancreatic islet α-cells exacerbates hyperglycemia in type 1 diabetes (T1D) and type 2 diabetes. Still, the underlying mechanistic pathways that regulate glucagon secretion remain controversial. Among the three complementary main mechanisms (intrinsic, paracrine, and juxtacrine) proposed to regulate glucagon release from α-cells, juxtacrine interactions are the least studied. It is known that tonic stimulation of α-cell EphA receptors by ephrin-A ligands (EphA forward signaling) inhibits glucagon secretion in mouse and human islets and restores glucose inhibition of glucagon secretion in sorted mouse α-cells, and these effects correlate with increased F-actin density. Here, we elucidate the downstream target of EphA signaling in α-cells. We demonstrate that RhoA, a Rho family GTPase, plays a key role in this pathway. Pharmacological inhibition of RhoA disrupts glucose inhibition of glucagon secretion in islets and decreases cortical F-actin density in dispersed α-cells and α-cells in intact islets. Quantitative FRET biosensor imaging shows that increased RhoA activity follows directly from EphA stimulation. We show that in addition to modulating F-actin density, EphA forward signaling and RhoA activity affect α-cell Ca^{2+} activity in a novel mechanistic pathway. Finally, we show that stimulating EphA forward signaling restores glucose inhibition of glucagon secretion from human T1D donor islets.

Diabetes is widely known as a disease of insulin, yet hyperglucagonemia and α-cell dysfunction also play an exacerbating role in the disease. Efforts in targeting glucagon for diabetes treatment have focused on glucagon receptor antagonists (1), although targeting glucagon secretion directly could offer an alternative therapeutic pathway. Moreover, it has been demonstrated that although therapeutics based on glucagon receptor antagonism restore euglycemia in patients with type 2 diabetes, they also lead to adverse effects (2,3). Hence, understanding the molecular mechanisms that regulate glucagon secretion in α-cells is of utmost importance to develop more effective therapeutics. The islet of Langerhans consists of different cell types, insulin-secreting β-cells, glucagon-secreting α-cells, and somatostatin-secreting δ-cells (4,5), and all of these cells show abnormal regulation of their hormone secretion following dispersion of the islet (6–9). Unlike insulin secretion from the β-cell, there is no consensus model for the regulation of glucagon secretion, so we need improved understanding of α-cell signaling pathways to identify potential therapeutic targets. Islet cells communicate through gap junctions, paracrine interactions, and juxtacrine cell contacts (4), and juxtacrine regulation remains the least studied mechanism. Juxtacrine signaling in α-cells comes primarily through direct contact with β-cells. In particular, the EphA/ephrin-A pathway has been shown to modulate glucagon secretion via α-cell EphA4 interactions with ephrin-A5 expressed on the surface of β-cells. Stimulation of EphA4 suppresses glucagon secretion by increasing cortical F-actin density (10).

β-Cells express both the receptor (EphA5) and ligand (ephrin-A5), but the α-cells express only receptors, primarily EphA4 but also smaller amounts of EphA7 (11,12), both of which bind to ephrin-A5 ligands on the β-cells. Therefore, the bidirectional signaling of the Eph/ephrin system, where stimulation of the Eph receptors by ephrin ligands results in "forward signaling," whereas stimulation of the ephrin ligands by Eph receptors leads to "reverse signaling," occurs in β-cells, while only the forward signaling applies to α-cells. In α-cells, stimulation of EphA4 forward signaling by ephrin-A5 Fc inhibits glucagon secretion (10). Inhibition of this forward signaling by either

Department of Cell Biology and Physiology, Washington University School of Medicine, St. Louis, MO

Corresponding author: David W. Piston, piston@wustl.edu

Received 18 November 2021 and accepted 26 July 2022

This article contains supplementary material online at https://doi.org/10.2337/figshare.20387091.

X.W.N. and Y.H.C. contributed equally to this work.

pharmacological inhibition or genetic knockout ($\alpha EphA4^{-/-}$) results in elevated glucagon secretion with no effect on insulin secretion (10). Stimulation of EphA4 forward signaling restores glucose inhibition of glucagon secretion in dispersed α-cells, providing a mechanism for the increased glucagon secretion and its impaired glucose inhibition observed when α-cells are removed from the islet environment. Similar to the putative EphA/ephrin-A regulatory pathway in β-cells (13), EphA4 signaling appears to modulate F-actin density to regulate glucagon secretion (10). Eph receptors modulate actin dynamics through Rho GTPase signaling in various cell types (14–16), and in β-cells, EphA5 signaling regulates insulin secretion through Rac1 activity (13). Bidirectional Eph/ephrin signaling in β-cells occurs through the modulation of Rac1 activity, where EphA forward signaling inhibits Rac1 activity, stimulates F-actin polymerization, and subsequently decreases insulin secretion, while ephrin-A reverse signaling stimulates Rac1 activity, reduces F-actin density, and consequently increases insulin secretion (13). Due to the similarities between α- and β-cells, we hypothesize that α-cell EphA4 also signals through Rho GTPases to regulate glucagon secretion. Here, we show that RhoA is the primary Rho-GTPase target downstream from α-cell EphA4 that is needed for proper glucose inhibition of glucagon secretion and that RhoA functions as a signaling hub that affects Ca^{2+} signaling, F-actin density modulation, and glucagon exocytosis.

RESEARCH DESIGN AND METHODS

Islet Isolation and Culture

All animal experiments were performed under approval of the Washington University Institutional Animal Care and Use Committee. As previously described, murine islets from adult male and female C57BL/6 mice (8–12 weeks old) were isolated using a 0.075% collagenase digestion at 34°C postpancreatectomy and cultured in islet media (RPMI 1640 with 10% FBS, 11 mmol/L glucose, and 1% penicillin-streptomycin) overnight before use (9). Note that we did not observe any sex-related differences in the results. Islets with α-cells expressing GCaMP6f were obtained by crossing mice expressing a Cre-dependent GCaMP6f (no. 028865; The Jackson Laboratory) with mice expressing GlucagoniCre (no. 030663; The Jackson Laboratory).

Human type 1 diabetes (T1D) islets were obtained through the Network for Pancreatic Organ donors with Diabetes (nPOD) and cultured in islet media overnight before use. Table 1 details islet donor information.

Table 1—Islet donor information

Donor	Age (years)	Sex	Years with T1D
1	19	Male	8
2	13	Female	7
3	10	Male	8

Islet Cell Dispersion

Islets were washed with Hanks' balanced salt solution (without Ca^{2+} or Mg^{2+}, pH 7.4; Gibco) and then dissociated in Accutase (Innovative Cell Technologies) for 15 min at 37°C with intermittent trituration. Dissociated cells were resuspended in islet culture media for subsequent use. For secretion assays, dispersed islet cells were placed in microcentrifuge tubes and glucagon levels in the supernatant and cells were measured as described in the hormone secretion assays section. For live cell imaging experiments, cells were plated on 5 μg/mL rhLaminin-521 (Gibco)–coated 35 mm glass bottom dishes (Cellvis). Plated cells were allowed to recover overnight prior to use.

Adenovirus Production and Transfection

Adenoviruses for the RhoA Förster resonance energy transfer (FRET) biosensor (plasmid obtained from Dr. Klaus Hahn, School of Medicine, University of North Carolina at Chapel Hill) and the Actin Chromobody (Chromotek) were produced with the AdEasy system (17). Dispersed islet cells were transduced with adenovirus resuspended in islet culture media the day after dispersion and incubated ∼16 h at 37°C, 5% CO_2. Intact islets were transduced with the RhoA FRET biosensor adenovirus in islet culture media and incubated for 24–48 h at 37°C, 5% CO_2. Cells were incubated in adenovirus-free islet culture media for a minimum of 3 h at 37°C, 5% CO_2, prior to experiments.

Hormone Secretion Assays

Islets and dispersed islet cells were treated as indicated with 4 μg/mL rodent ephrin-A5 Fc (R&D Systems), 100 μmol/L Rhosin hydrochloride, 200 μg/mL NSC23766 (Tocris Bioscience), 20 μg/mL ML141(MilliporeSigma), or vehicle (PBS or DMSO, 0.05%; Sigma-Aldrich) and incubated for 1 h at 37°C in serum-free islet culture media. Samples were then equilibrated in Krebs-Ringer bicarbonate HEPES buffer (KRBH) buffer (128.8 mmol/L NaCl, 4.8 mmol/L KCl, 1.2 mmol/L KH_2PO_4, 1.2 mmol/L $MgSO_4$, 2.5 mmol/L $CaCl_2$, 20 mmol/L HEPES, and 5 mmol/L $NaHCO_3$, pH 7.4) with 0.1% BSA and 2.8 mmol/L glucose for 30 min at 37°C with continuation of the appropriate treatments. Either intact islets or dispersed cells were incubated in 100 μL KRBH buffer at low (1 mmol/L) or high (11 mmol/L) glucose with the treatment condition in microcentrifuge tubes for 45 min at 37°C. For intact islets, the supernatant was collected, and islets were transferred to microcentrifuge tubes containing 100 μL acidified ethanol solution (1.5% HCl in 70% ethanol) to lyse the cells for hormone content. For dispersed cells, the supernatant was collected and replaced with nonionic lysis buffer (50 mmol/L Tris, pH 7.4; 150 mmol/L NaCl; 1% Triton X-100 plus 5 μg/mL aprotinin; and 45 mmol/L phenylmethylsulfonyl fluoride) for hormone content. Glucagon and insulin were measured by Lumit Glucagon and Insulin Immunoassays (Promega), respectively, and somatostatin was measured with ELISA (Phoenix Pharmaceuticals Inc.). Data are presented as

percent total hormone content to normalize for sample differences.

Live-Cell Imaging

Plated islets or monodispersed islet cells were equilibrated on a heated, CO_2-controlled microscope stage of a Zeiss LSM880 confocal microscope with use of a Plan-Apochromat 63× 1.4 NA oil immersion objective at 37°C, 5% CO_2, in KRBH with 2.8 mmol/L glucose for 15 min. Buffer was then switched to KRBH buffer either containing 1 mmol/L or 11 mmol/L glucose followed by another 30 min equilibration at 37°C, 5% CO_2. An initial baseline image time course was acquired followed by the respective treatment conditions with 4 μg/mL ephrin-A5 Fc, 250 μmol/L Rhosin, 12.5 μmol/L 4-(2,5-dimethyl-pyrrol-1-yl)-2-hydroxy-benzoic acid (DPHBA) (Santa Cruz Biotechnology) or vehicle (DMSO), a 1 h incubation, and further image acquisition. For FRET imaging experiments, the biosensor signals, mCerulean3 and YPet, were measured with LSM 880 spectral detector mode with 458 nm excitation. The entire emission spectrum was measured for each pixel, resulting in a spatial-spectral datacube (x, y, λ—the two-dimensional image across all measured wavelengths). The composite spectral signal was linearly unmixed into the two FRET component signals with the ZEISS ZEN imaging software. For Ca^{2+} imaging experiments, GCaMP6f fluorescence was measured with 488 nm laser excitation, detected at an emission range of 490–597 nm with the spectral detector.

Fixed-Cell and Islet Immunofluorescence Imaging

Dispersed islet cells or whole islets were cultured overnight on coverslips coated with 5 μg/mL rhLaminin-521 (Gibco) or gelatin solution (Sigma-Aldrich), respectively. Coverslips with dispersed islet cells were treated with Rhosin (100 μmol/L) or rodent ephrin-A5 Fc (4 μg/mL) in serum-free RPMI media containing 11 mmol/L glucose for 1 h, washed twice in RPMI, and cultured in KRBH containing 2.8 mmol/L glucose for 30 min. Thereafter, dispersed islet cells were treated either with Rhosin (100 μmol/L) or ephrin-A5 Fc (4 μg/mL) in KRBH containing 1 mmol/L or 11 mmol/L glucose for 45 min. For increasing penetration of Rhosin into islets, whole islets were treated with Rhosin (100 μmol/L) in serum-free RPMI media containing 2.8 mmol/L glucose for 3 h. Whole islets were then treated with Rhosin (100 μmol/L) in serum-free RPMI media containing 1 mmol/L or 11 mmol/L glucose for 1 h. In some experiments, cells were treated in a sequentially ordered manner by 1-h treatment with Rhosin followed by 1-h treatment with ephrin-A5 Fc (in either 1 mmol/L or 11 mmol/L glucose) or in reverse order. Dispersed islet cells were fixed and permeabilized at room temperature using 2% paraformaldehyde for 20 min followed by 0.1% Triton X-100 in PBS for 5 min. After 1-h incubation in blocking buffer (2% BSA in PBS containing 0.05% Tween20), cells were washed in PBS. Immunostaining was performed with primary antibodies against glucagon (1:100, GLUN F7; AvantGen) and F-actin (4:100, ab205; Abcam) at 4°C overnight, followed by incubation in a mixture of secondary antibodies (1:1,000, Alexa Fluor 488 goat anti-rabbit, A-21094, Molecular Probes, and 1:1,000, Alexa Fluor 568 goat anti-mouse, A11057, Invitrogen) for 1 h. For whole islets, fixation and permeabilization were conducted at room temperature using 2% paraformaldehyde for 20 min followed by 0.1% Tween20 in PBS for 1 h. Following 1-h incubation in blocking buffer (2% BSA in PBS containing 0.05% Tween20), islets were washed in PBS. Immunostaining was performed with primary antibodies against glucagon (1:100, GLUN F7; AvantGen) at 4°C overnight, followed by incubation in secondary antibodies (1:1,000, Alexa Fluor 488 goat anti-rabbit, A-21094; Molecular Probes) for 90 min. Subsequently, islets were stained for F-actin (1:1,000, Phalloidin 555; Thermo Fisher Scientific) for 15 min, followed by DAPI staining (1:1,000) at room temperature for 10 min. Stained cells or islets were mounted in ProLong antifade and imaged on the Zeiss LSM880 microscope with a Plan-Apochromat 63× 1.4 NA objective lens and dual-band dichroic filter set for 488 nm/561 nm laser excitation. For imaging DAPI in whole islets, 405 nm laser excitation was used. For each condition, 25–30 fields of views were collected with an average of three to five cells or one islet per field of view. For quantification of F-actin intensity, a region of interest is manually drawn around each cell and the average intensity is measured with ImageJ. Intensity values are then normalized to cell area.

Data Analysis and Statistics

Data were analyzed with Microsoft Excel, ImageJ, MATLAB, and GraphPad Prism. FRET data are shown as percent change in acceptor-to-donor ratio pre- and posttreatment. Actin data are shown as average intensity normalized to cell area. Time series Ca^{2+} images were converted into kymographs, the number of peaks were counted using a peak finding script available in MATLAB, and data are shown as average frequency of Ca^{2+} influx events before and after treatment. Data are reported as either mean ± SEM or mean ± SD. Statistical significance was assessed as described in the figure captions.

Data and Resource Availability

The data set generated during or analyzed during the current study is available from the corresponding author on reasonable request.

RESULTS

RhoA Inhibition Impairs Glucose Inhibition of Glucagon Secretion in Pancreatic Islet

EphA5/ephrin-A5 in β-cells modulates insulin secretion by signaling through Rac1 (13). Given the many similarities between β- and α-cells, we hypothesized that Rac1 or another Rho GTPase would mediate EphA4 activation effects on glucagon secretion in the α-cell. We focused on

well-characterized Rho GTPases through pharmacological inhibition of RhoA, Cdc42, and Rac1 by Rhosin (18), ML141 (19), and NSC23766 (20), respectively. Rhosin is a specific small-molecule RhoA inhibitor that inhibits guanine nucleotide exchange factor (GEF)-catalyzed RhoA activation (18). ML141 is a selective inhibitor of Cdc42 that decreases GTP binding to Cdc42 (19), and NSC23766 inhibits Rac1 by binding to GEFs and blocking Rac1 activation (20). We measured insulin, glucagon, and somatostatin secretion from islets at 1 mmol/L and 11 mmol/L glucose in the presence and absence of each inhibitor (Fig. 1). In islets, RhoA inhibition resulted in the loss of glucose dependence of glucagon secretion, while inhibition of Cdc42 and Rac1 did not significantly affect the glucose dependence of glucagon secretion (Fig. 1*A*). RhoA inhibition also greatly increased insulin secretion at both low and high glucose concentrations, while inhibition of Cdc42 and Rac1 had minimal effect on glucose-stimulated insulin secretion from islets (Fig. 1*B*). Cdc42 inhibition raised somatostatin secretion at low glucose, while Rac1 and RhoA inhibition elevated somatostatin secretion at both glucose levels (Fig. 1*C*). One concern would be that the effects of Rho GTPase inhibition on the α-cell are indirect and governed by the β- or δ-cells. However, the effect of increased somatostatin and/or insulin is decrease in glucagon secretion, so we would expect inhibition of glucagon based on the data in Fig. 1*B* and *C*. Instead, we see significantly increased glucagon secretion with RhoA inhibition, even though somatostatin and/or insulin levels were increased, supporting a key role for this GTPase in mediating α-cell glucagon secretion. We tested the role of RhoA activity in whole islets by measuring F-actin intensities of immunostained α-cells (Supplementary Fig. 1). These data show a significant decrease of F-actin intensities in the Rhosin-treated groups (both 1 mmol/L and 11 mmol/L glucose), indicating that RhoA activity affects F-actin polymerization.

EphA4 Forward Signaling Stimulates RhoA

RhoA inhibition appears to block the effects of EphA forward signaling in α-cells. In testing the relationship between EphA receptor activation and RhoA activity, we used a FRET biosensor to report on RhoA activity in α-cells (21). In this biosensor, an increased FRET reflects increased RhoA activity (Fig. 2*A*). To identify α-cells, we use a fluorescent protein (FP) reporter expressed under a Cre-lox system triggered by the glucagon promoter that leads to tandem dimer-red fluorescent protein (tdRFP) expression specifically in α-cells (8,9). This results in robust tdRFP expression for easy identification of α-cells, either within the islet or when cells are dispersed, as we describe here.

Following biosensor expression via adenoviral transduction, the acceptor and donor intensities were measured by spectral imaging (Fig. 2*B*) before and after treatment with ephrin-A5 Fc and Rhosin at 1 mmol/L and 11 mmol/L glucose (Fig. 2*C*). Treatment with ephrin-A5 Fc resulted in an increased acceptor-to-donor intensity ratio under both glucose conditions, consistent with EphA4 signaling to RhoA. As a control, application of Rhosin to inhibit RhoA activity resulted in a decreased FRET ratio (Fig. 2*C*). For better understanding of the relationship between stimulation of EphA forward signaling and RhoA activity, sequential treatments with Rhosin and ephrin-A5 Fc were conducted on dispersed α-cells (Fig. 2*D*). When dispersed α-cells were pretreated with ephrin-A5 Fc, which is expected to stimulate RhoA activity, the effects of Rhosin on RhoA activity were diminished. In contrast, pretreatment with Rhosin greatly reduced the action of ephrin-A5 Fc (Fig. 2*D*), as observed in the decreased percentage change in acceptor-to-donor intensity ratio as compared with treatment with

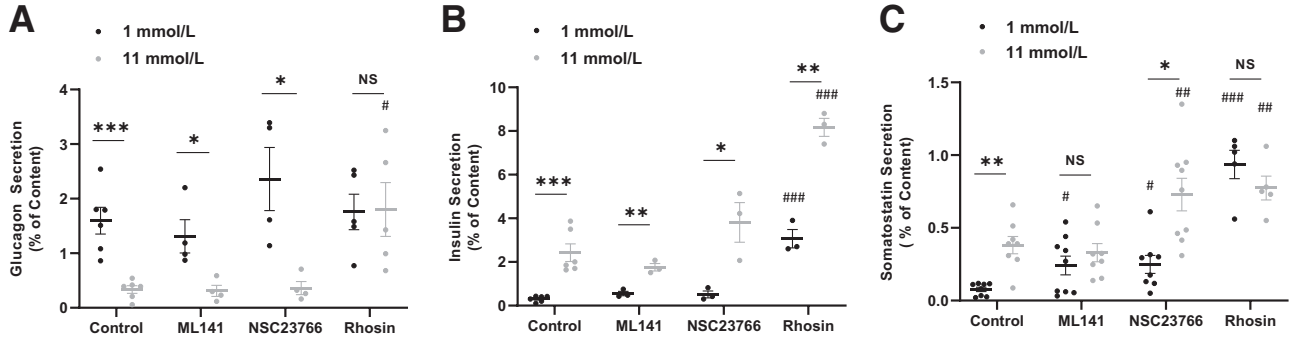

Figure 1— RhoA inhibition disrupts the glucose-dependent inhibition of glucagon secretion. Glucagon (*A*), insulin (*B*), and somatostatin (*C*) secretions were measured in mouse islets treated with control (PBS or DMSO), 50 μmol/L ML141 (Cdc42 inhibitor), 400 μmol/L NSC23766 (Rac1 inhibitor), or 100 μmol/L Rhosin (RhoA inhibitor), respectively, under 1 mmol/L (black circles) or 11 mmol/L (gray circles) glucose conditions. Data are represented as mean ± SEM ($n > 4$ experiments). * above lines represents significant differences between the same condition at low and high glucose as determined with Student *t* test: *$P < 0.05$, **$P < 0.01$, ***$P < 0.001$. # directly above columns represents statistical differences between condition and control at the same glucose concentration as determined with Student *t* test: #$P < 0.05$, ##$P < 0.01$, ###$P < 0.001$.

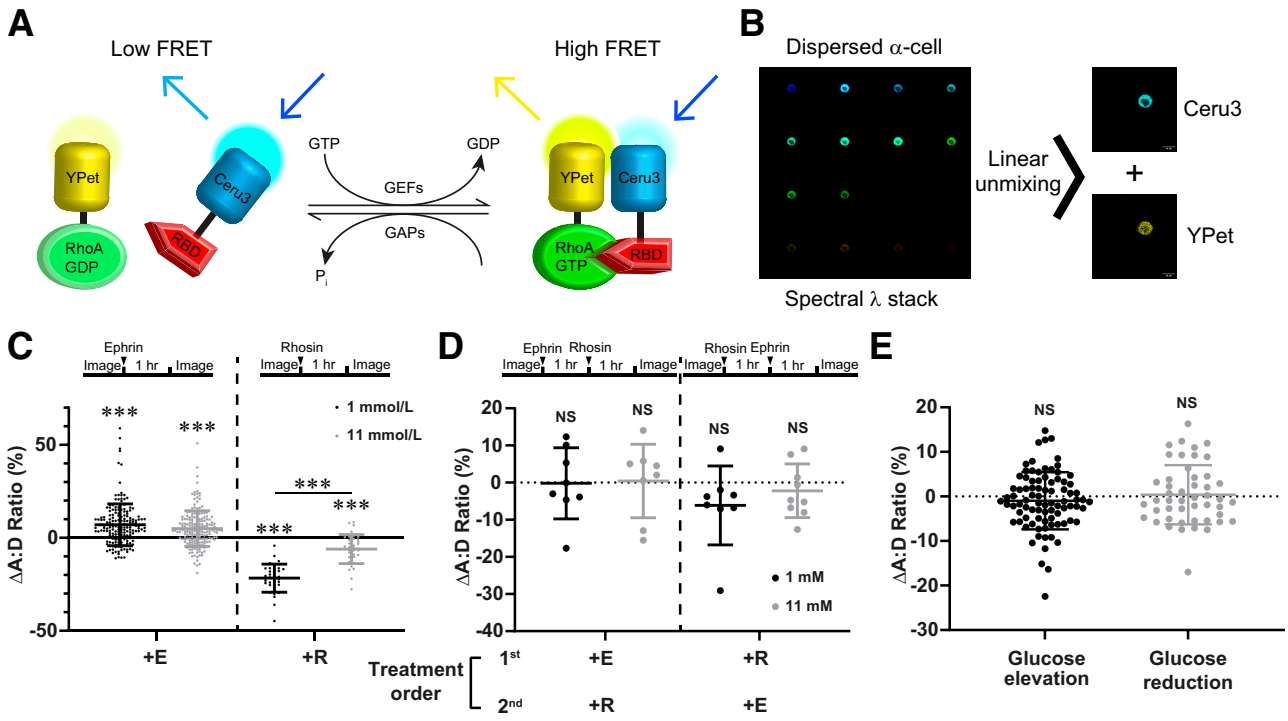

Figure 2—EphA forward signaling stimulates RhoA activity. *A*: Schematic of RhoA FRET biosensor. In the inactive state, as facilitated by the conversion of RhoA-GTP to RhoA-GDP through GTPase-activating proteins (GAPs), acceptor (YPet)-labeled RhoA does not bind to donor (mCerulean3)-labeled RBD, resulting in a low FRET state. On activation of RhoA by GEFs, the change in conformation of RhoA allows for the binding of RBD to RhoA, resulting in a high FRET state. *B*: Dispersed α-cells transfected with the RhoA FRET sensor were imaged with confocal microscopy. Spectral stacks were collected and linearly unmixed to obtain the donor and acceptor intensities. *C*: The changes in the acceptor-to-donor intensity ratio before and after treatment (either with 4 μg/mL ephrin-A5 Fc [+E] or 250 μmol/L Rhosin [+R]) at low (black circles) and high (gray circles) glucose concentrations were measured and are reported as % changes. *D*: The changes in the acceptor-to-donor intensity ratio on sequential treatments (ephrin-A5–Fc–Rhosin/Rhosin–ephrin-A5–Fc) at low (black circles) and high (gray circles) glucose concentrations. *E*: % changes in the acceptor-to-donor intensity ratio on switching glucose concentrations from 1 mmol/L to 11 mmol/L (glucose elevation) and 11 mmol/L to 1 mmol/L (glucose reduction). Data presented as mean ± SD ($n \geq 8$ cells, maximum 193). One-sample *t* test and unpaired *t* test were used to determine statistical significance between no treatment value (0% change in acceptor-to-donor intensity ratio) and treatment conditions, and the same treatment condition at low and high glucose, respectively. ***$P < 0.001$. hr, hour; NS, $P > 0.05$.

ephrin-A5 Fc only (Fig. 2*C*). These data suggest that EphA forward signaling competes with Rhosin in modulating RhoA activity. In comparison with the changes seen following EphA receptor stimulation or RhoA inhibition, changes in the glucose concentration had minimal effect on RhoA activity (Fig. 2*E*). It should be noted that glucose blunts the inhibitory effect of Rhosin (Fig. 2*C*) on RhoA activity. This is likely due to glucose effects on RhoA signaling that are independent of EphA receptors, such as cAMP-mediated pathways (22–27). We next tested the effects of EphA forward signaling, Rhosin inhibition of RhoA activity, and changes in glucose concentration on the RhoA activity of α-cells in intact mouse islets. Treatment with ephrin-A5 Fc resulted in a trend toward increased acceptor-to-donor intensity ratio under both glucose conditions, while treatment with Rhosin led to a trend toward reduced acceptor-to-donor intensity ratio (Supplementary Fig. 2*A*), comparable with the results in dispersed α-cells (Fig. 2*C*). Similar to dispersed α-cells, changes in the glucose concentration had minimal effect on RhoA activity of α-cells in intact mouse islets (Supplementary Fig. 2*B*).

Inhibition of RhoA Decouples EphA Activation From F-Actin Polymerization

In α-cells, EphA/ephrin-A signaling correlates with changes in F-actin density (10), and RhoA modulates F-actin formation in other cell types (28). To determine the role of EphA receptors and RhoA in modulating F-actin density in α-cells, we performed immunofluorescence experiments on dispersed α-cells to visualize F-actin density and correlated this to glucagon secretion from the same cell population prior to fixation (Fig. 3). Treatment with Rhosin reduced F-actin density at both 1 and 11 mmol/L glucose (Fig. 3*A–D* and *I*), similar to what we observed in whole islets (Supplementary Fig. 1), which also resulted in increased glucagon secretion (Fig. 3*J*). As expected from previous work (10), application of ephrin-A5 Fc both increased F-actin density (Fig. 3*E–H* and *K*) and decreased glucagon secretion (Fig. 3*L*). To test directly the role of RhoA in the pathway between EphA stimulation and F-actin polymerization, we treated dispersed α-cells sequentially with Rhosin and ephrin-A5 Fc (Supplementary Fig. 3). Pretreatment with Rhosin eliminated ephrin-A5 Fc stimulation of F-actin

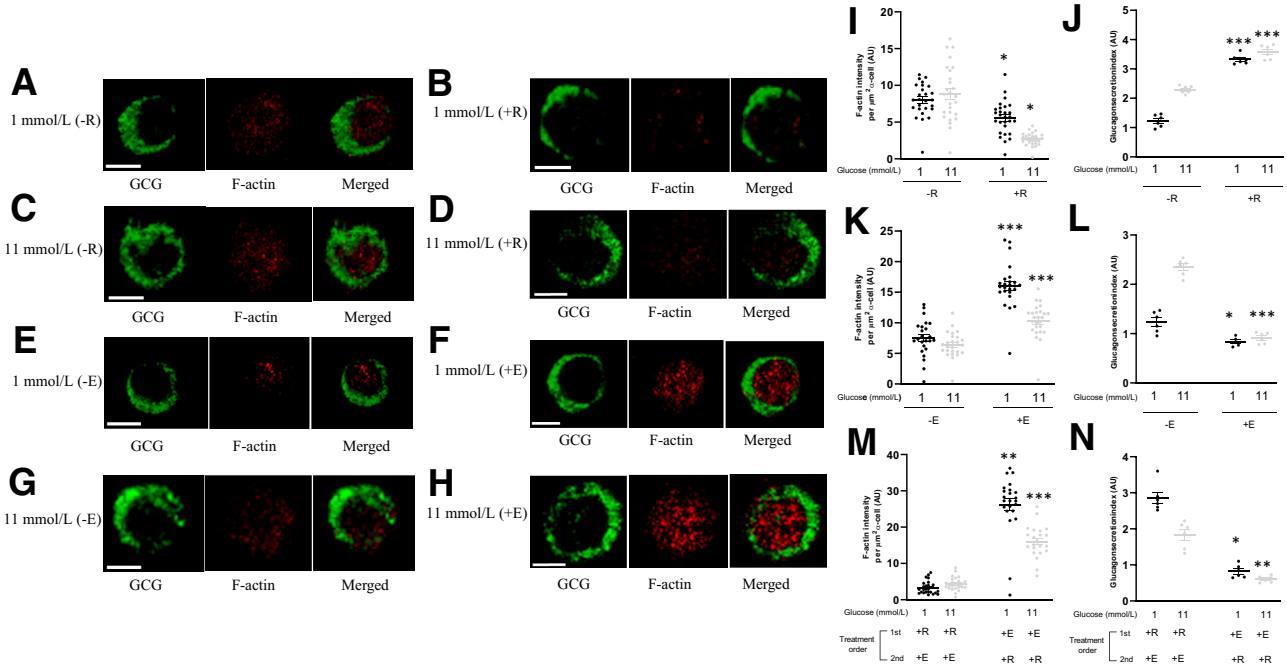

Figure 3—Ephrin-A5 enhances F-actin intensities and suppresses glucagon secretion in α-cells, while Rhosin reduces F-actin intensities and increases glucagon secretion. Dispersed islet cells of mice (n = 4–6) treated with Rhosin (+R) (100 μmol/L) or ephrin-A5 Fc (+E) (4 μg/mL) in low glucose (1 mmol/L) or high glucose (11 mmol/L) conditions. Cells were immunostained with antibodies against glucagon (GCG) and F-actin. Confocal immunofluorescent images show a typical α-cell in low glucose vs. high glucose conditions in the absence (*A* and *C*) and presence (*B* and *D*) of Rhosin or in the absence (*E* and *G*) and presence (*F* and *H*) of ephrin-A5 Fc (10 μm scale bars). F-actin intensities of the cell in response to Rhosin (*I* and *J*), ephrin-A5 Fc (*K* and *L*), or sequential treatments (Rhosin–ephrin-A5–Fc/ephrin-A5–Fc–Rhosin) (*M* and *N*), with measurement in both low and high glucose conditions. Statistical differences between each treatment and its corresponding control or between sequential treatment orders were determined by unpaired t test or Mann-Whitney U statistical test at $\alpha = 0.05$ (*$P < 0.05$, **$P < 0.01$, ***$P < 0.001$). Values expressed as mean ± SEM. AU, arbitrary units.

density and kept glucagon secretion at high levels (Fig. 3*M* and *N*). Similarly, pretreatment with ephrin-A5 Fc kept F-actin density high and glucagon secretion low (Fig. 3*M* and *N*). These data are consistent with long-lived effects of F-actin polymerization that are not undone by inhibition of RhoA. In contrast, inhibiting RhoA with Rhosin treatment before ephrin-A5 Fc stimulation blocks the coupling between EphA receptor activation, F-actin polymerization, and reduced glucagon secretion.

Inhibition of RhoA Increases Ca^{2+} Activity in α-Cells

Because Rho GTPases are known to affect multiple signaling pathways, we tested whether the EphA/ephrin-A juxtacrine regulatory pathway engages in cross talk with the intrinsic/electrophysiological regulatory pathway through RhoA. Since the influx of calcium ions is a necessary trigger for vesicle exocytosis, Ca^{2+} is a good surrogate reporter of α-cell electrophysiology that may affect glucagon secretion. To test for effects of RhoA activity on α-cell electrophysiology, we used the Cre-dependent GCaMP6f FP-based sensor (29) mice crossed with Glucagon-iCre mice (30) to visualize Ca^{2+} dynamics specifically in α-cells.

We measured changes in Ca^{2+} activity upon RhoA inhibition in islets from these animals and observed Ca^{2+} influx events as bursts of fluorescence (Fig. 4*A*). The time-series fluorescence traces for each α-cell were converted to kymographs, where each peak in the kymographs represents an individual burst of Ca^{2+} influx events. Pharmacological inhibition of RhoA by Rhosin resulted in an increase in Ca^{2+} activity compared with the control under low glucose condition (Fig. 4*B*). We also tested the effects of inhibiting EphA forward signaling on Ca^{2+} activity through pharmacological inhibition of EphA receptors by DPHBA, which disrupts suppression of glucagon secretion in islets (10). Inhibition of EphA forward signaling led to an increase in Ca^{2+} activity as compared with the control at low glucose concentration. Control measurements were conducted in the same sequence as Rhosin/DPHBA treatment but with application only of the DMSO vehicle instead.

Stimulation of EphA Forward Signaling Restores Glucose-Dependent Inhibition of Glucagon Secretion in Human T1D Donor Islets

We next examined the role of EphA/ephrin-A signaling in the context of human T1D. Using valuable donor islets from individuals with T1D, we were able to observe the effect of EphA forward signaling on glucagon secretion in donor islets from patients with T1D (Fig. 5). These islets do not contain functional β-cells (verified by insulin secretion

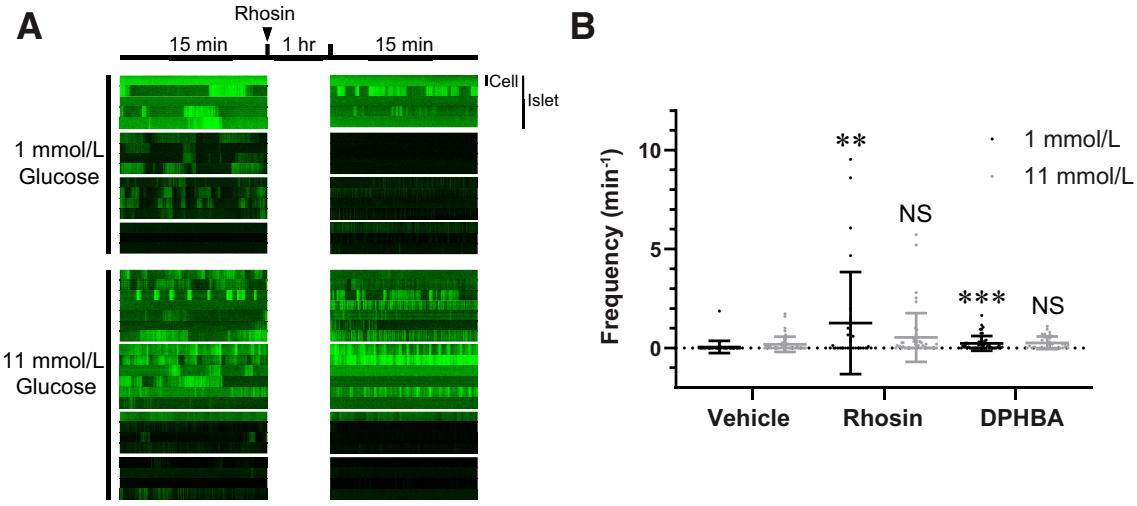

Figure 4—RhoA inhibition by Rhosin increases α-cell calcium activity in intact mouse islets. *A*: Representative kymographs of GCaMP6 fluorescence detected in 16–21 individual α-cells within four GCG-iCre-GCaMP6 mouse islets under 1 or 11 mmol/L glucose exposure, before and after Rhosin treatment. *B*: Treatment with 250 μmol/L Rhosin and 12.5 μmol/L DPHBA significantly elevated overall calcium frequency as compared with treatment with vehicle (DMSO) under low glucose concentration (1 mmol/L). Such increase is less significant under high glucose concentration (11 mmol/L). Data presented as mean ± SD (1 mmol/L glucose, DMSO, three islets, 37 cells; 11 mmol/L glucose, DMSO, five islets, 50 cells; 1 mmol/L glucose, Rhosin, six islets, 29 cells; 11 mmol/L glucose, Rhosin, seven islets, 47 cells; 1 mmol/L glucose, DPHBA, three islets, 48 cells; 11 mmol/L glucose, DPHBA, three islets, 34 cells). Statistical significance between different drug treatments and vehicle of the same glucose concentration was determined using a Kolmogorov-Smirnov test. ***$P < 0.001$; **$P < 0.01$. hr, hour; NS, $P > 0.05$.

measurements, where these islets had no measurable insulin secretion [data not shown]), which is expected to result in a loss of juxtacrine signaling that depends on α-/β-cell contacts. Thus, we expect the α-cells in these islets to behave more like dispersed cells than those within a nondiabetic islet. Consistent with previous data from dispersed human α-cells (9), glucagon secretion from these T1D donor human islets show increased glucagon secretion with rising glucose concentration. In agreement with our hypothesis, treating these T1D islets with ephrin-A5 Fc restores glucose-dependent inhibition of glucagon secretion (Fig. 5*B*). While the normal glucose-dose response is restored, we do not observe the overall suppression of glucagon secretion that is expected based on the dispersed α-cell results (Fig. 3*L*).

DISCUSSION

The molecular mechanisms that regulate glucagon secretion in α-cells remain controversial, but recent advances have led to three main groups of models: *1*) intrinsic α-cell mechanisms, *2*) paracrine interactions, and *3*) juxtacrine interactions (4). While these models are not mutually exclusive and may indeed work synergistically to control glucagon exocytosis, our understanding of juxtacrine pathways is the least well developed. Toward better understanding of this coupling mechanism, we examined the signaling pathway downstream of EphA receptor activation in pancreatic islet α-cells by focusing on Rho GTPases, which are established targets of Eph receptors. We showed that different Rho GTPase family members appear to have distinct functions in the islet. In α-cells, inhibition of RhoA activity uniquely disrupts glucose control of glucagon secretion from islets (Fig. 1) and dispersed cells (Fig. 3). In contrast, blocking Cdc42 and Rac1 does not show the same effect (Fig. 1). It is worth noting that despite an increase in insulin and somatostatin secretions with RhoA inhibition in islets, glucagon secretion is significantly increased with RhoA inhibition, indicating a major role of RhoA in EphA/ephrin-A juxtacrine signaling in α-cells that outweighs the effects of paracrine inhibition. Forward signaling through EphA receptors following ephrin-A5 Fc treatment stimulates RhoA activity (Fig. 2), and inhibition of RhoA decouples EphA forward signaling from F-actin polymerization (Fig. 3). Taken together, these data provide strong evidence of RhoA as the key downstream effector of EphA4/7 receptors in α-cells and are consistent with RhoA serving as the major link between EphA signaling and increased F-actin density.

Rho GTPases are well-characterized downstream signaling targets of Eph receptors (16,31,32), so we focused on this signaling pathway. We found that RhoA activity disrupts glucose-mediated inhibition of glucagon secretion from islets, while Cdc42 and Rac1 do not. RhoA activity showed minimal change upon change in glucose concentrations in the case of both the ephrin-A5 Fc treatment and glucose controls (Fig. 2*C* and *E*). These data suggest that RhoA activity is independent of glucose, which is consistent with its signaling downstream of EphA receptors. RhoA inhibition is also able to block the effects of ephrin-A5 in dispersed α-cells (Fig. 3), further demonstrating

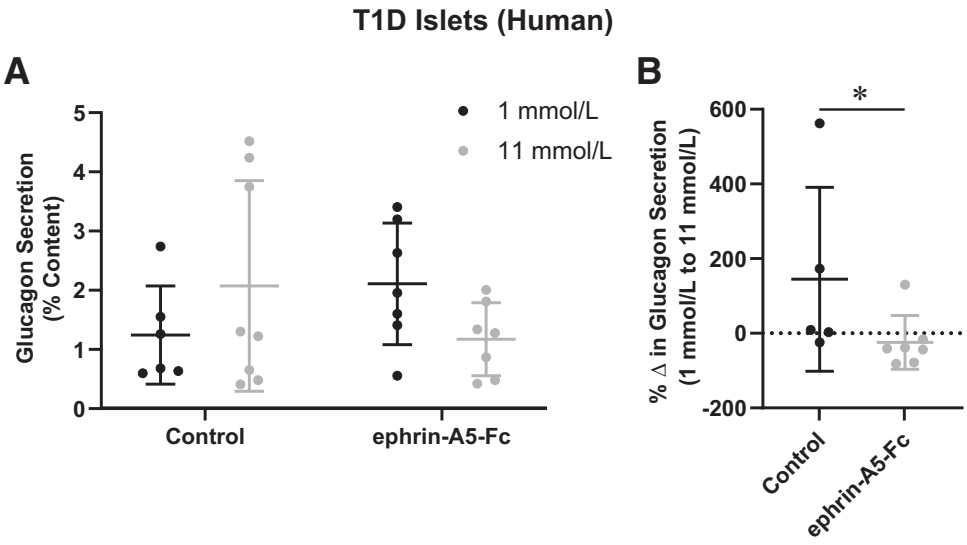

Figure 5—Stimulation of EphA forward signaling restores glucose-dependent glucagon secretion in T1D islets. *A*: Glucagon secretion measured in human T1D islets not treated (control) and treated with ephrin-A5 Fc under low (black circles) and high (gray circles) glucose conditions. *B*: % change in glucagon secretion from 1 mmol/L to 11 mmol/L glucose for both control islets and ephrin-A5 Fc–treated islets. Data represented as mean ± SD (n = 7–8 technical replicates obtained using ~300 islets from three donors). Statistical significance was determined with a Mann-Whitney U test. *$P < 0.05$.

RhoA signaling as part of the EphA/ephrin-A pathway. To investigate directly the activation of RhoA by the EphA/ephrin-A juxtacrine signaling pathway in α-cells, we used a FRET-based biosensor that reports RhoA activity by the binding of donor-labeled Rho binding domain (RBD) to acceptor-labeled RhoA upon RhoA activation (Fig. 2*A*) (21). The resulting data provide direct evidence supporting RhoA as a key intermediary in the signaling pathway from EphA to F-actin formation. We performed quantitative FRET experiments using spectral imaging to eliminate signal cross talk between the donor and acceptor FPs (33). By using spectral imaging and linear unmixing, we can quantify the donor and acceptor individual FP components free of spectral bleed-through artifacts (Fig. 2*B*). The FRET data show directly the activation of RhoA by EphA receptor stimulation in dispersed α-cells and that such EphA forward signaling–mediated activation of RhoA can be blocked by Rhosin. This is consistent with data on the relationship between EphA stimulation and RhoA activity reported using other cellular systems (14,34,35).

F-actin plays a critical role in the proposed model of EphA/ephrin-A regulation of glucagon secretion, putatively by cortical F-actin forming a physical barrier to exocytosis (10). We demonstrated that RhoA inhibition results in decreased F-actin density and subsequent increase in glucagon secretion in dispersed α-cells (Fig. 3), directly in line with the role of RhoA as a downstream effector of EphA/ephrin-A signaling. However, the actin network is a highly important and dynamic region involved in all aspects of the lifetime of a vesicle, from trafficking to docking to exocytosis (36), with many different proteins involved in this process chain. Showing a central role of RhoA signaling in α-cell juxtacrine regulation should facilitate investigation of downstream effectors and elucidate the molecular mechanisms underlying F-actin's effect on exocytosis. For example, one well-characterized downstream effector of RhoA is Rho-associated kinase (ROCK) (37). Characterization of such mechanisms and their specific roles will contribute to better understanding of glucagon secretion regulation and provide additional therapeutic targets.

Rho GTPases signal through many downstream effectors, so we investigated whether RhoA controls aspects of α-cell function other than cortical F-actin formation. We showed that EphA forward signaling and RhoA are involved not only in the modulation of F-actin but also in the electrophysiology of the α-cell (Fig. 4). To our knowledge, these are the first data looking at this pathway in the α-cell. We assayed Ca^{2+} activity by measuring the frequency of Ca^{2+} influx events, which increases following RhoA inhibition or EphA inhibition. These data suggest that EphA receptor activation may inhibit glucagon secretion not only through changes in F-actin but also through decreased Ca^{2+} activity. EphA forward signaling and RhoA activation affect Ca^{2+} activity more significantly at 1 mmol/L glucose than 11 mmol/L glucose, possibly due to the fact that glucagon secretion is high under low glucose conditions and any changes in the α-cell glucagon secretion pathway will be accentuated at low glucose levels. However, Ca^{2+} activity changes can be difficult to interpret, as the data show significant heterogeneity, consistent with previous reports (8,38,39). The underlying causes and functional importance of this heterogeneity remain unknown, but inhibition of

RhoA or EphA signaling does not appreciably change the amount of heterogeneity (Fig. 4).

There are many potential mechanisms by which RhoA activity controls ion channel activity. RhoA signaling has been shown to inhibit voltage-dependent delayed rectifying potassium (K_{DR}) channels by both direct binding (40) and by an actin polymerization–dependent uridine triphosphate (UTP) pathway (41). Further, RhoA and Rac1 have been implicated in regulating the trafficking of K^+ channels to the membrane (42,43). RhoA has also been shown to inhibit Na^+ channels (44,45) and *L*-type Ca^{2+} channels in cardiac myocytes (46). How RhoA activity might affect ion channel activity in the α-cell is currently unknown.

The resulting model of RhoA as a signaling hub in the α-cell is shown in Fig. 6. Based on the data provided here, we propose that RhoA is a critical downstream target of the EphA/ephrin-A juxtacrine signaling pathway in α-cells. EphA receptor activation was previously shown to modulate F-actin density and subsequently inhibit glucagon release (10). Here, we have demonstrated the role of RhoA activity as a key point in this pathway. We have also shown that RhoA activation reduces α-cell Ca^{2+} activity, and this also suppresses glucagon secretion. In these ways, RhoA acts as a negative regulator of glucagon secretion in α-cells through EphA forward signaling. The targets of elevated RhoA activity are cortical F-actin polymerization and intracellular Ca^{2+} activity. In this manuscript, we have shown data supporting the link between RhoA signaling and electrophysiological regulation of glucagon secretion, but RhoA might also interact with another α-cell second messenger, cAMP (22,23). In epithelial-like and neuroblastoma cell lines, RhoA activation counteracts cAMP-induced changes in cell morphology (24), and cAMP has been reported to regulate RhoA in many studies (25–27). If this interaction held true in α-cells, this would effectively intertwine the known paracrine interactions to the juxtacrine regulatory system.

Importantly, we observed restored glucose inhibition of glucagon secretion in human donor islets from patients with T1D upon stimulation of EphA forward signaling (Fig. 5). As T1D results in loss of β-cells, juxtacrine signaling that depends on an interface between α- and β-cells is lost. Consistent with previous work on sorted mouse

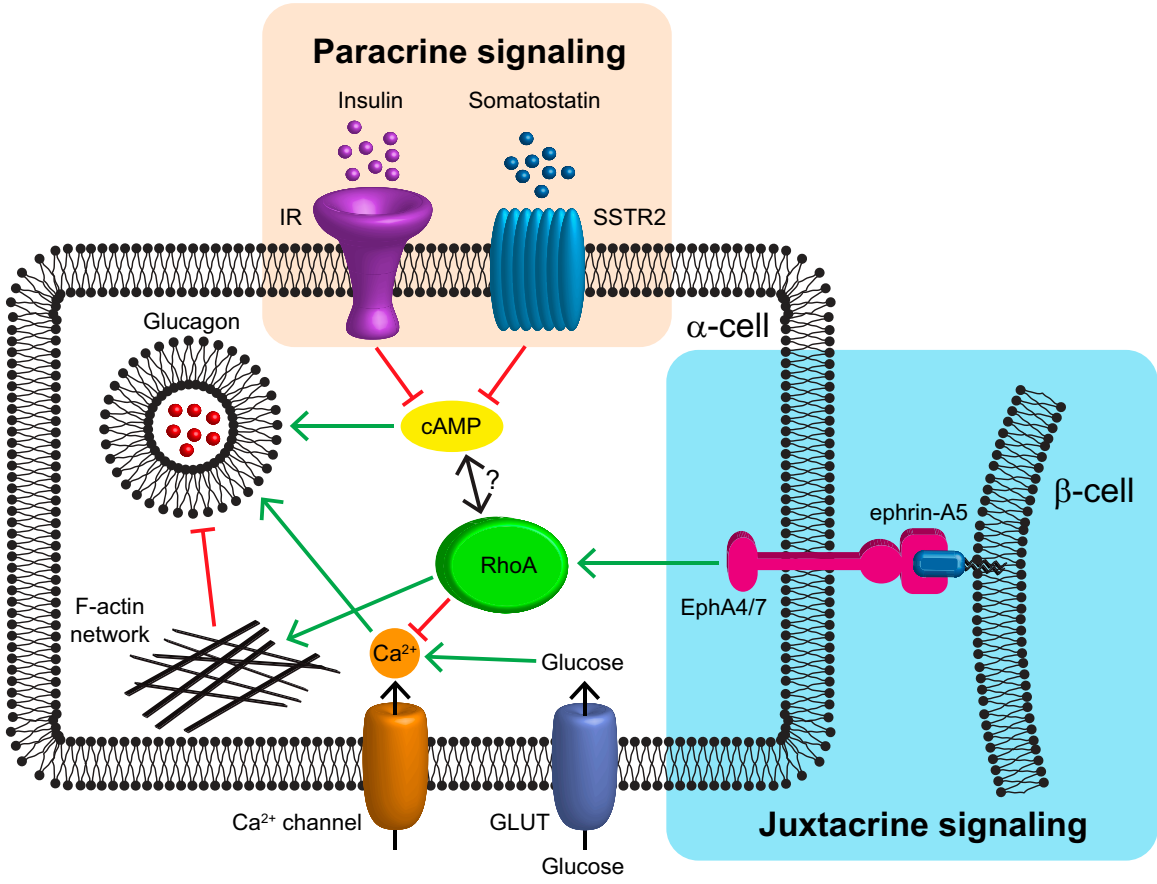

Figure 6—Proposed model with RhoA as the signaling hub for regulation of glucagon secretion in α-cells. RhoA is involved in the EphA/ephrin-A juxtacrine signaling pathway in α-cells by modulating F-actin density and subsequently inhibiting glucagon release. Furthermore, RhoA activation also leads to reduced α-cell Ca^{2+} activity, which results in suppressed glucagon secretion. Overall, RhoA acts as a negative regulator of glucagon secretion in α-cells through EphA forward signaling, Ca^{2+} channel activity, and possibly cAMP pathways.

α-cells (10), treatment with ephrin-A5 Fc was able to restore the glucose-dependent inhibition of glucagon secretion in T1D islets, even though overall glucagon secretion levels were comparable with those of the untreated islets. A life-threatening concern for patients with diabetes is hypoglycemia, where blood glucose levels fall dangerously below the standard range (<70 mg/dL). The ability to restore proper glucose-regulated glucagon secretion by stimulation of EphA forward signaling presents a potential therapeutic avenue for treating hypoglycemic conditions with EphA agonists in T1D patients. Conversely, EphA inhibition was demonstrated to enhance glucose-stimulated insulin secretion in mouse and human islets, and improve glucose tolerance in mice, highlighting a potential therapeutic treatment for type 2 diabetes (47). The potential of treating both T1D and type 2 diabetes by targeting EphA signaling may provide a versatile approach into clinical applications. Hyperglucagonemia is a hallmark in diabetes as well as dispersed α-cells, so these data suggest that dysregulation of other regulatory pathways in T1D islets might interfere with EphA/ephrin-A-dependent restriction of glucagon secretion. In that case, stimulation of EphA forward signaling in T1D islet α-cells may not be sufficient to ameliorate hyperglucagonemia despite its ability to do so in murine α-cells (10). Of course, these data could also be an artifact of small sample size due to the limited availability of T1D islets.

Acknowledgments. The authors thank Dr. Klaus Hahn (School of Medicine, University of North Carolina at Chapel Hill) for providing the RhoA FRET biosensor plasmid. The authors thank Dr. Rita Bottino at the University of Pittsburgh and the nPOD donor screening program for providing the isolated T1D human donor islets.

Funding. This research was supported by the National Institutes of Health (NIH) (grants R01DK123301 and R01DK115972), The Leona M. and Harry B. Helmsley Charitable Trust (G-1912-03558 and G-2001-04215), and the Washington University Center for Cellular Imaging supported in part by the Washington University Diabetes Research Center (NIH grant P30DK020579). T1D donor islet isolation was also supported by The Leona M. and Harry B. Helmsley Charitable Trust (G-2018PG-T1D027).

Duality of Interest. No potential conflicts of interest relevant to this article were reported.

Author Contributions. X.W.N., Y.H.C., A.U., and D.W.P. planned the research. X.W.N., Y.H.C., F.A., C.K., and A.U. performed experiments and analysis. X.W.N., Y.H.C., and D.W.P. wrote the first draft of the manuscript, which was edited and approved by all authors. D.W.P. is the guarantor of this work and, as such, had full access to all the data in the study and takes responsibility for the integrity of the data and the accuracy of the data analysis.

References

1. Christensen M, Bagger JI, Vilsbøll T, Knop FK. The alpha-cell as target for type 2 diabetes therapy. Rev Diabet Stud 2011;8:369–381

2. Guzman CB, Zhang XM, Liu R, et al. Treatment with LY2409021, a glucagon receptor antagonist, increases liver fat in patients with type 2 diabetes. Diabetes Obes Metab 2017;19:1521–1528

3. Kazda CM, Frias J, Foga I, et al. Treatment with the glucagon receptor antagonist LY2409021 increases ambulatory blood pressure in patients with type 2 diabetes. Diabetes Obes Metab 2017;19:1071–1077

4. Ng XW, Chung YH, Piston DW. Intercellular communication in the islet of Langerhans in health and disease. Compr Physiol 2021;11:2191–2225

5. Da Silva Xavier G. The cells of the islets of langerhans. J Clin Med 2018;7:54

6. Lernmark A. The preparation of, and studies on, free cell suspensions from mouse pancreatic islets. Diabetologia 1974;10:431–438

7. Bennett BD, Jetton TL, Ying G, Magnuson MA, Piston DW. Quantitative subcellular imaging of glucose metabolism within intact pancreatic islets. J Biol Chem 1996;271:3647–3651

8. Le Marchand SJ, Piston DW. Glucose suppression of glucagon secretion: metabolic and calcium responses from α-cells in intact mouse pancreatic islets. J Biol Chem 2010;285:14389–14398

9. Reissaus CA, Piston DW. Reestablishment of glucose inhibition of glucagon secretion in small pseudoislets. Diabetes 2017;66:960–969

10. Hutchens T, Piston DW. EphA4 receptor forward signaling inhibits glucagon secretion from α-cells. Diabetes 2015;64:3839–3851

11. Dorrell C, Schug J, Lin CF, et al. Transcriptomes of the major human pancreatic cell types. Diabetologia 2011;54:2832–2844

12. Li J, Klughammer J, Farlik M, et al. Single-cell transcriptomes reveal characteristic features of human pancreatic islet cell types. EMBO Rep 2016;17:178–187

13. Konstantinova I, Nikolova G, Ohara-Imaizumi M, et al. EphA-Ephrin-A-mediated β cell communication regulates insulin secretion from pancreatic islets. Cell 2007;129:359–370

14. Shamah SM, Lin MZ, Goldberg JL, et al. EphA receptors regulate growth cone dynamics through the novel guanine nucleotide exchange factor ephexin. Cell 2001;105:233–244

15. Bisson N, Poitras L, Mikryukov A, Tremblay M, Moss T. EphA4 signaling regulates blastomere adhesion in the Xenopus embryo by recruiting Pak1 to suppress Cdc42 function. Mol Biol Cell 2007;18:1030–1043

16. Noren NK, Pasquale EB. Eph receptor-ephrin bidirectional signals that target Ras and Rho proteins. Cell Signal 2004;16:655–666

17. Luo J, Deng ZL, Luo X, et al. A protocol for rapid generation of recombinant adenoviruses using the AdEasy system. Nat Protoc 2007;2:1236–1247

18. Shang X, Marchioni F, Sipes N, et al. Rational design of small molecule inhibitors targeting RhoA subfamily Rho GTPases. Chem Biol 2012;19:699–710

19. Surviladze Z, Waller A, Strouse JJ, et al. A potent and selective inhibitor of Cdc42 GTPase. In *Probe Reports from the NIH Molecular Libraries Program*. Bethesda, MD, National Center for Biotechnology Information, 2010

20. Gao Y, Dickerson JB, Guo F, Zheng J, Zheng Y. Rational design and characterization of a Rac GTPase-specific small molecule inhibitor. Proc Natl Acad Sci U S A 2004;101:7618–7623

21. Pertz O, Hodgson L, Klemke RL, Hahn KM. Spatiotemporal dynamics of RhoA activity in migrating cells. Nature 2006;440:1069–1072

22. Elliott AD, Ustione A, Piston DW. Somatostatin and insulin mediate glucose-inhibited glucagon secretion in the pancreatic α-cell by lowering cAMP. Am J Physiol Endocrinol Metab 2015;308:E130–E143

23. Yu Q, Shuai H, Ahooghalandari P, Gylfe E, Tengholm A. Glucose controls glucagon secretion by directly modulating cAMP in alpha cells. Diabetologia 2019;62:1212–1224

24. Dong JM, Leung T, Manser E, Lim L. cAMP-induced morphological changes are counteracted by the activated RhoA small GTPase and the Rho kinase ROKalpha. J Biol Chem 1998;273:22554–22562

25. Chen Y, Wang Y, Yu H, Wang F, Xu W. The cross talk between protein kinase A- and RhoA-mediated signaling in cancer cells. Exp Biol Med (Maywood) 2005;230:731–741

26. Jones SE, Palmer TM. Protein kinase A-mediated phosphorylation of RhoA on serine 188 triggers the rapid induction of a neuroendocrine-like phenotype in prostate cancer epithelial cells. Cell Signal 2012;24:1504–1514

27. Oishi A, Makita N, Sato J, Iiri T. Regulation of RhoA signaling by the cAMP-dependent phosphorylation of RhoGDIα. J Biol Chem 2012;287:38705–38715

28. Machacek M, Hodgson L, Welch C, et al. Coordination of Rho GTPase activities during cell protrusion. Nature 2009;461:99–103
29. Chen TW, Wardill TJ, Sun Y, et al. Ultrasensitive fluorescent proteins for imaging neuronal activity. Nature 2013;499:295–300
30. Shiota C, Prasadan K, Guo P, Fusco J, Xiao X, Gittes GK. Gcg^{CreERT2} knockin mice as a tool for genetic manipulation in pancreatic alpha cells. Diabetologia 2017;60:2399–2408
31. Zhou L, Martinez SJ, Haber M, et al. EphA4 signaling regulates phospholipase Cgamma1 activation, cofilin membrane association, and dendritic spine morphology. J Neurosci 2007;27:5127–5138
32. Fukata M, Kaibuchi K. Rho-family GTPases in cadherin-mediated cell-cell adhesion. Nat Rev Mol Cell Biol 2001;2:887–897
33. Dickinson ME, Bearman G, Tille S, Lansford R, Fraser SE. Multi-spectral imaging and linear unmixing add a whole new dimension to laser scanning fluorescence microscopy. Biotechniques 2001;31:1272–1278, 1274–1276, 1278
34. Rottner K, Hall A, Small JV. Interplay between Rac and Rho in the control of substrate contact dynamics. Curr Biol 1999;9:640–648
35. Fu AKY, Hung KW, Huang H, et al. Blockade of EphA4 signaling ameliorates hippocampal synaptic dysfunctions in mouse models of Alzheimer's disease. Proc Natl Acad Sci U S A 2014;111:9959–9964
36. Li P, Bademosi AT, Luo J, Meunier FA. Actin remodeling in regulated exocytosis: toward a mesoscopic view. Trends Cell Biol 2018;28:685–697
37. Amano M, Nakayama M, Kaibuchi K. Rho-kinase/ROCK: a key regulator of the cytoskeleton and cell polarity. Cytoskeleton (Hoboken) 2010;67:545–554
38. Le Marchand SJ, Piston DW. Glucose decouples intracellular Ca2+ activity from glucagon secretion in mouse pancreatic islet alpha-cells. PLoS One 2012;7:e47084
39. Li J, Yu Q, Ahooghalandari P, et al. Submembrane ATP and Ca2+ kinetics in α-cells: unexpected signaling for glucagon secretion. FASEB J 2015;29:3379–3388
40. Cachero TG, Morielli AD, Peralta EG. The small GTP-binding protein RhoA regulates a delayed rectifier potassium channel. Cell 1998;93:1077–1085
41. Luykenaar KD, El-Rahman RA, Walsh MP, Welsh DG. Rho-kinase-mediated suppression of KDR current in cerebral arteries requires an intact actin cytoskeleton. Am J Physiol Heart Circ Physiol 2009;296:H917–H926
42. Boyer SB, Slesinger PA, Jones SVP. Regulation of Kir2.1 channels by the Rho-GTPase, Rac1. J Cell Physiol 2009;218:385–393
43. Stirling L, Williams MR, Morielli AD. Dual roles for RHOA/RHO-kinase in the regulated trafficking of a voltage-sensitive potassium channel. Mol Biol Cell 2009;20:2991–3002
44. Abramochkin DV, Filatova TS, Pustovit KB, Dzhumaniiazova I, Karpushev AV. Small G-protein RhoA is a potential inhibitor of cardiac fast sodium current. J Physiol Biochem 2021;77:13–23
45. Staruschenko A, Nichols A, Medina JL, Camacho P, Zheleznova NN, Stockand JD. Rho small GTPases activate the epithelial Na(+) channel. J Biol Chem 2004;279:49989–49994
46. Yatani A, Irie K, Otani T, Abdellatif M, Wei L. RhoA GTPase regulates L-type Ca2+ currents in cardiac myocytes. Am J Physiol Heart Circ Physiol 2005;288:H650–H659
47. Jain R, Jain D, Liu Q, et al. Pharmacological inhibition of Eph receptors enhances glucose-stimulated insulin secretion from mouse and human pancreatic islets. Diabetologia 2013;56:1350–1355